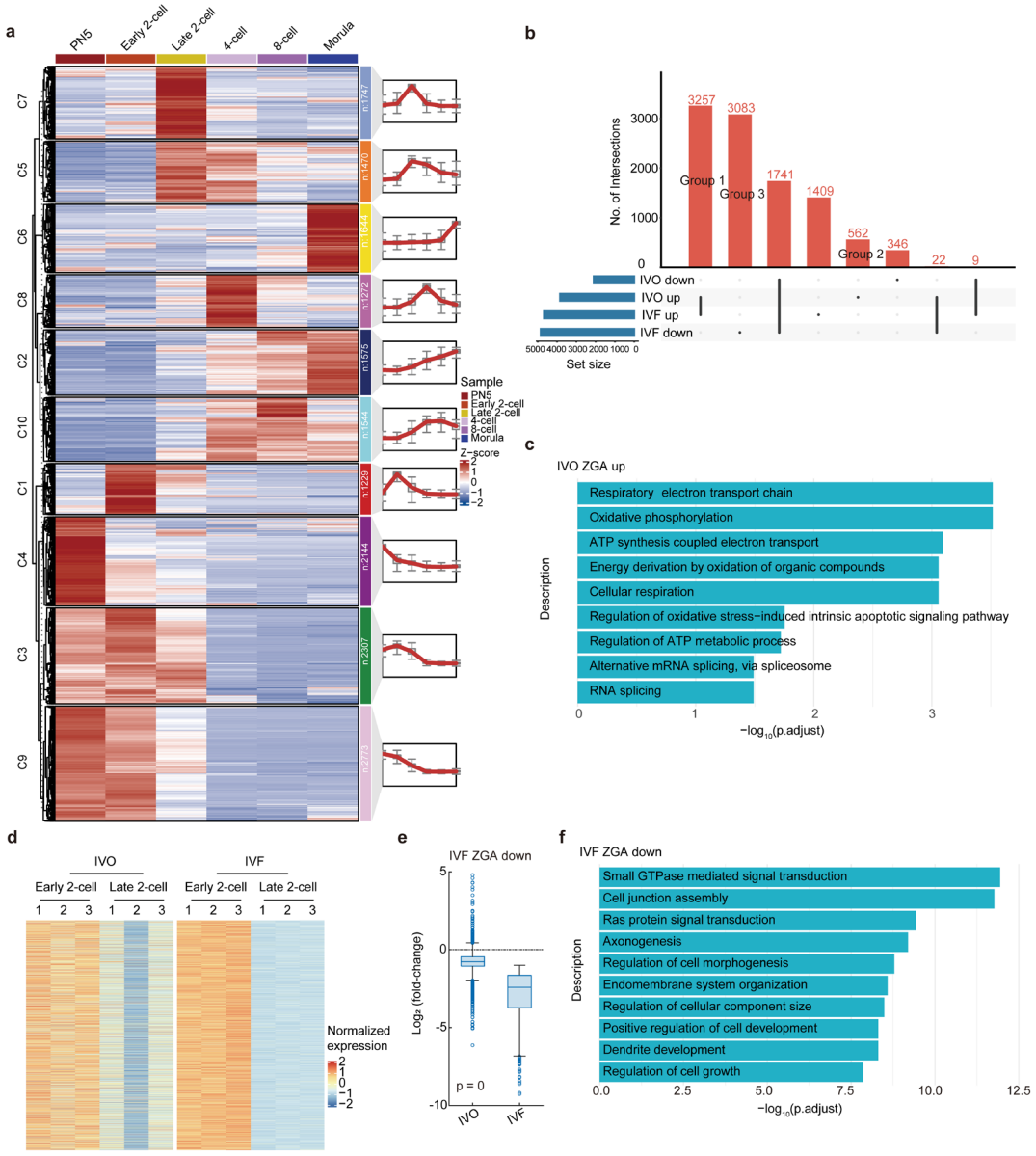

Supplementary Figure 1. Transcriptional differences between IVF- and IVO-conceived embryos from PN5 to morula. (a) Expression heatmap showing the 10 clusters we identified based on transcription data of IVO-conceived embryos. Genes with maximal TPM values > 1 were included for

clustering. **(b)** Overlap of DEGs during ZGA process following IVF/IVO. **(c)** Functions of group 2 genes. P-adjust was calculated based on hypergeometric distribution with BH (Benjamini-Hochberg) correction. **(d)-(e)** Heatmap **(d)** and boxplot **(e)** showing the expression variation of group 3 genes during ZGA following IVO/IVF. N = 3083. T-test (both-tail) was performed. The line inside of each box is the sample median and the top and bottom edges of each box are the 0.75 and 0.25 quartiles, respectively. The distance between the top and bottom edges is the interquartile range (IQR). The whiskers are lines that extend above and below each box within 1.5 times the IQR and outliers are values that are more than 1.5 times the IQR away from the top or bottom of the box. **(f)** Functions of group 3 genes. P-adjust was calculated based on hypergeometric distribution with BH (Benjamini-Hochberg) correction.

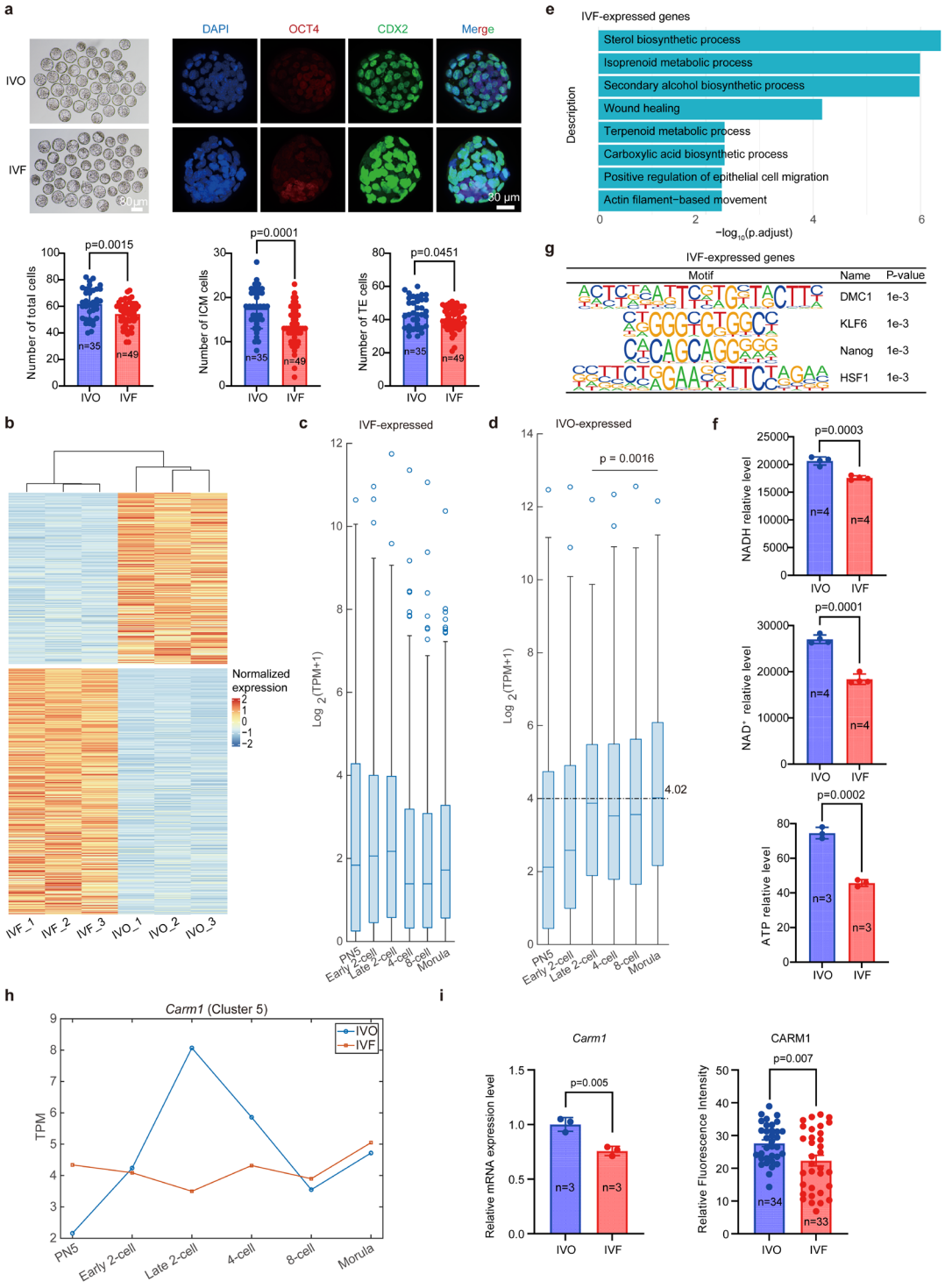

Supplementary Figure 2. Transcriptional differences between IVF- and IVO-conceived blastocysts. (a) Upper: Representative light microscopy and immunofluorescence images of the EPI markers OCT4 (red), the TE markers CDX2 (green) and nuclear stain DAPI (blue) in mouse blastocysts conceived

from IVO and IVF. Scale bars, 30 μm; lower: quantification of the number of total, ICM and TE cells in mouse blastocysts conceived from IVO and IVF. Source data are provided as a Source Data file. Error bar: mean±std. Two-tailed unpaired t tests were performed. **(b)** Expression heatmap showing the DEGs (IVO-expressed or IVF-expressed genes) identified based on the transcription data of IVF- and IVO-conceived blastocysts. **(c)-(d)** The transcription variation of IVF-expressed **(c)** and IVO-expressed **(d)** genes shown in (**b**) from PN5 to morula. T-test (both-tail) was performed. The line inside of each box is the sample median and the top and bottom edges of each box are the 0.75 and 0.25 quartiles, respectively. The distance between the top and bottom edges is the interquartile range (IQR). The whiskers are lines that extend above and below each box within 1.5 times the IQR and outliers are values that are more than 1.5 times the IQR away from the top or bottom of the box. **(e)** Functions of IVF-expressed genes. P-adjust was calculated based on hypergeometric distribution with BH (Benjamini-Hochberg) correction. **(f)** The levels of NADH, NAD+ and ATP in IVF- and IVO-conceived blastocysts. Source data are provided as a Source Data file. Error bar: mean ± std. Two-tailed unpaired t tests were performed. **(g)** Sequence motif analysis on the promoter regions of IVF-expressed genes. P-values were obtained based on hypergeometric distribution. **(h)** The transcription dynamics of *Carm1* from PN5 to morula following IVF or IVO. **(i)** Left: Relative mRNA expression level of *Carm1* in late 2-cell following IVF or IVO. Right: Relative fluorescence intensity of CARM1 in late 2-cell following IVF or IVO. Source data are provided as a Source Data file. Error bar: mean ± std. Two-tailed unpaired t tests were performed.

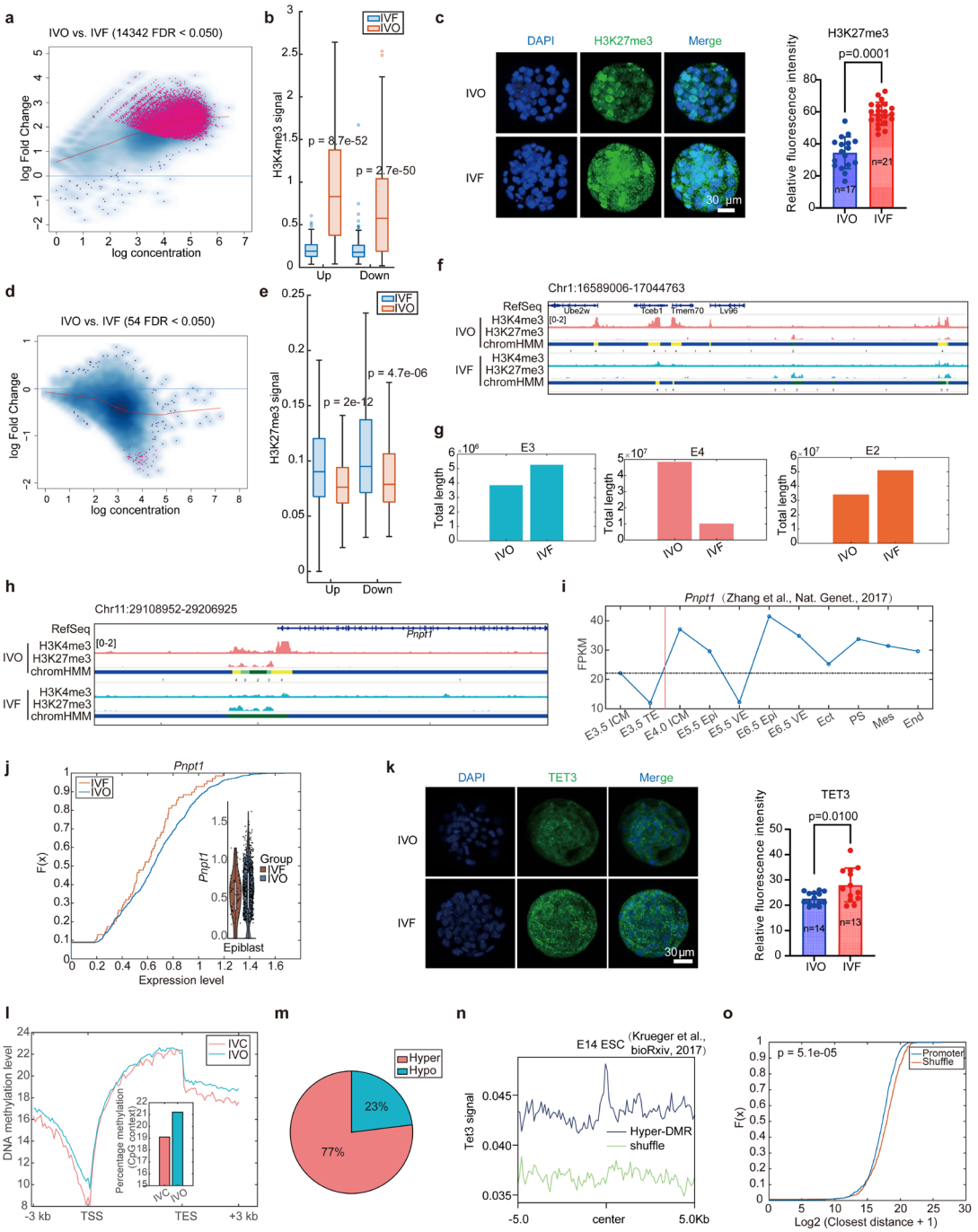

Supplementary Figure 3. Epigenetic differences between IVF- and IVO-conceived blastocysts. (a) MA-plot showing the differentially H3K4me3-binding regions. **(b)** The H3K4me3 signal within promoter regions of DEGs in IVF- and IVO-conceived blastocysts. T-test (both-tail) was performed. The line

inside of each box is the sample median and the top and bottom edges of each box are the 0.75 and 0.25 quartiles, respectively. The distance between the top and bottom edges is the interquartile range (IQR). The whiskers are lines that extend above and below each box within 1.5 times the IQR and outliers are values that are more than 1.5 times the IQR away from the top or bottom of the box. **(c)** Staining and quantification for H3K27me3 in IVF- and IVO-conceived blastocysts. Scale bar, 30 μm. Source data are provided as a Source Data file. Error bar: mean±std. Two-tailed unpaired t tests were performed. **(d)** MA-plot showing the differentially H3K27me3-binding regions (n = 2 biological replicates for each condition). **(e)** The H3K27me3 signal within promoter regions of DEGs in IVF- and IVO-conceived blastocysts. T-test (both-tail) was performed. The line inside of each box is the sample median and the top and bottom edges of each box are the 0.75 and 0.25 quartiles, respectively. The distance between the top and bottom edges is the interquartile range (IQR). The whiskers are lines that extend above and below each box within 1.5 times the IQR and outliers are values that are more than 1.5 times the IQR away from the top or bottom of the box. **(f)** A snapshot showing the distribution of H3K4me3, H3K27me3 and chromatin states identified via chromHMM in IVF- and IVO-conceived blastocysts. **(g)** The genome length of chromatin states 2, 3 and 4 identified based on chromHMM. **(h)** The distribution of H3K4me3, H3K27me3 and chromatin states around the promoter regions of *Pnpt1*. **(i)** The expression level of *Pnpt1* in several cell types (Epi, epiblast; VE, visceral endoderm; Ect, ectoderm; End, endoderm; Mes, mesoderm; PS, primitive streak). Expression data of *Pnpt1* was downloaded from GEO (Gene Expression Omnibus) under the accession number GSE76505. **(j)** Cumulative distribution of *Pnpt1* expression level in ~E6.5 epiblast following IVF/IVO at single-cell level. Inner panel: violin-plots showing the expression level of *Pnpt1* in IVF- and IVO-conceived ~E6.5 epiblast. **(k)** Staining and quantification for TET3 in IVF- and IVO-conceived blastocysts. Scale bar, 30 μm. Source data are provided as a

Source Data file. Error bar: mean ± std. Two-tailed unpaired t tests were performed. **(l)** The methylation level between IVC- (*in vivo* fertilization and *in vitro* culture) and IVO-conceived embryos. **(m)**The percentage of hyper- and hypo-DMR. **(n)** The distribution of Tet3 signal around hyper-DMRs and randomly selected regions. Tet3 ChIP-seq data were downloaded from GEO (Gene Expression Omnibus) under the accession number GSE94688. (**o**) Cumulative distribution of the distance between promoters of DEGs or randomly selected genes and its closest DMRs. Welch's unequal variance t-test (both-tail) was performed.

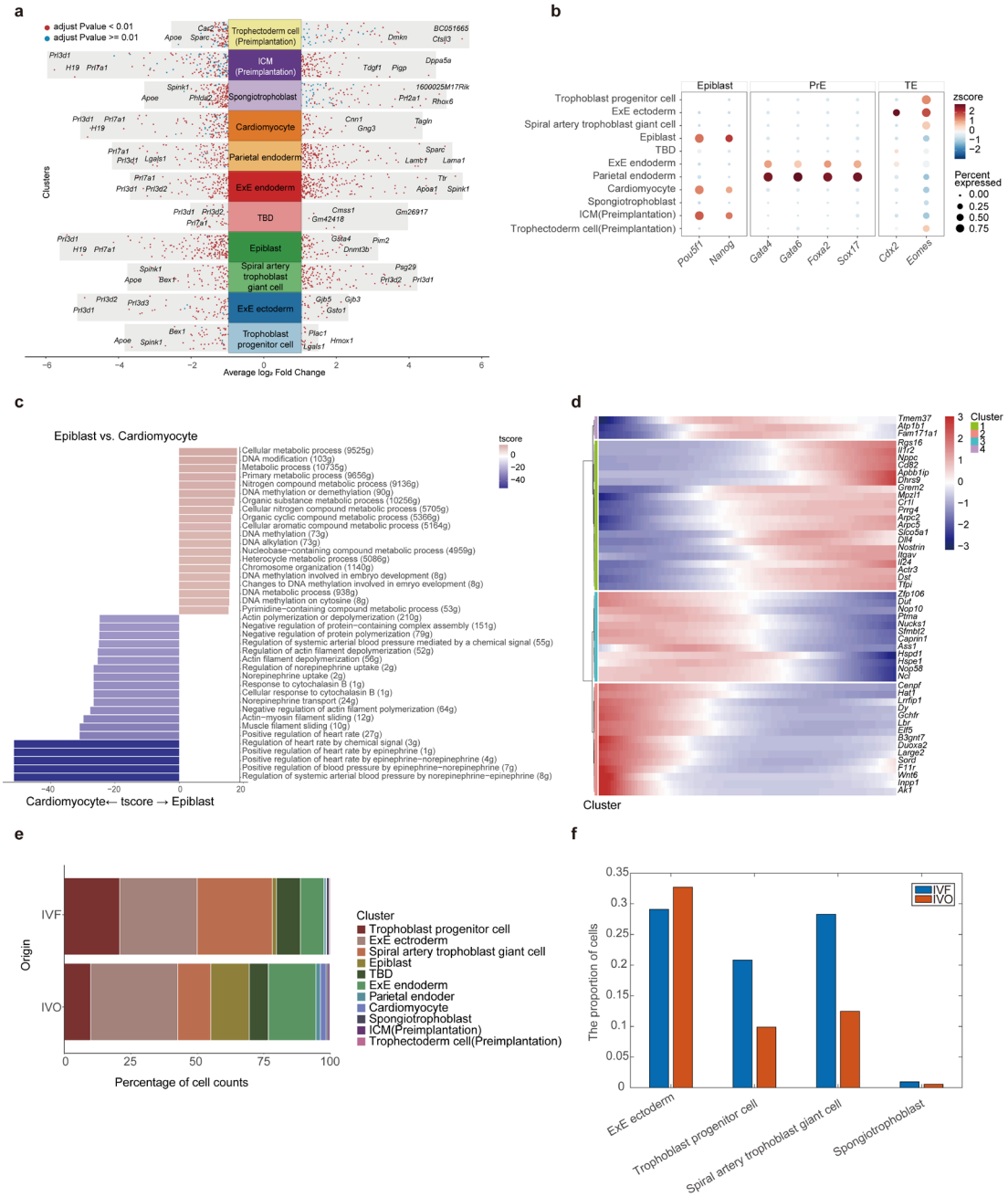

Supplementary Figure 4. scRNA-seq data revealing the abnormal cell compositions in IVF-conceived post-implantation embryos. (a) Volcano plots showing the specific genes of each cell type. **(b)** Dotplot summarizing the expression of marker genes in each cell type. **(c)** Waterfall-plot showing the GO

terms enriched in epiblast or cardiomyocyte. **(d)** Transcriptional variation of dynamics genes along the pseudotime. **(e-f)** The percentage of each cell type **(e)** and four cell types related to placenta development **(f)** in IVF- and IVO-conceived embryos.

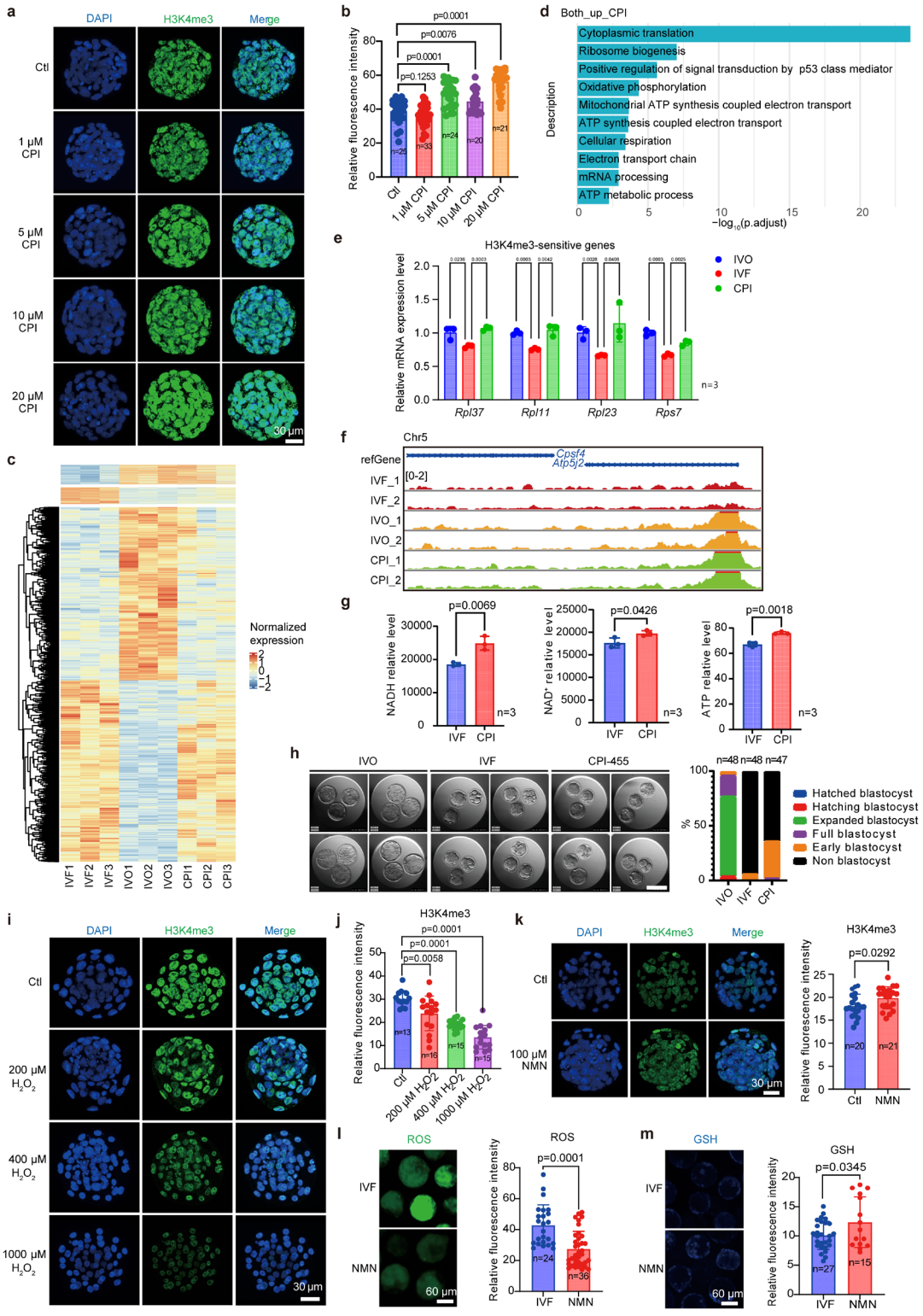

Supplementary Figure 5. The effects of CPI-455 supplementation on mouse embryo development. (a) Representative immunofluorescence images of H3K4me3 in several conditions with different CPI-455 concentrations.

Scale bar, 30 μm. **(b)** The fluorescence intensity of H3K4me3 in several conditions with different CPI-455 concentrations. Source data are provided as a Source Data file. Error bar: mean ± std. Two-tailed unpaired t tests were performed. **(c)** The expression level of DEGs ($p < 0.05$) between IVF- and IVO-conceived blastocysts in IVF-, IVO- and CPI-treated blastocysts. **(d)** Functions of both-up genes, which belong to SRGs. P-adjust was calculated based on hypergeometric distribution with BH (Benjamini-Hochberg) correction. **(e)** The relative mRNA expression level of several SRGs related to "positive regulation of signal transduction by p53 class mediator". Source data are provided as a Source Data file. Error bar: mean ± std. Two-tailed unpaired t tests were performed. **(f)** An example showing the dynamic H3K4me3 variation at *Atp5j2* promoter regions, which was closely related to its transcription. **(g)** The levels of NADH, NAD+ and ATP in IVF-conceived blastocysts with/without CPI-455 treatment. Source data are provided as a Source Data file. Error bar: mean± std. Two-tailed unpaired t tests were performed. **(h)** The proportion of blastocyst in E3.5 under several conditions including IVO, IVF and CPI-455. Source data are provided as a Source Data file. **(i-j)** Staining **(i)** and quantification **(j)** for H3K4me3 under several conditions with different concentrations of H_2O_2. Scale bar, 30 μm. Source data are provided as a Source Data file. Error bar: mean± std. Ordinary one-way ANOVA were performed. **(k)** Staining and quantification for H3K4me3 in IVF-conceived embryos with/without NMN treatment. Scale bar, 30 μm. Source data are provided as a Source Data file. Error bar: mean±std. Two-tailed unpaired t tests were performed. **(l)-(m)** Staining and quantification for ROS **(l)** and GSH **(m)** in IVF-conceived blastocysts with/without NMN treatment. Scale bars, 60 μm. Source data are provided as a Source Data file. Error bar: mean±std. Two-tailed unpaired t tests were performed.

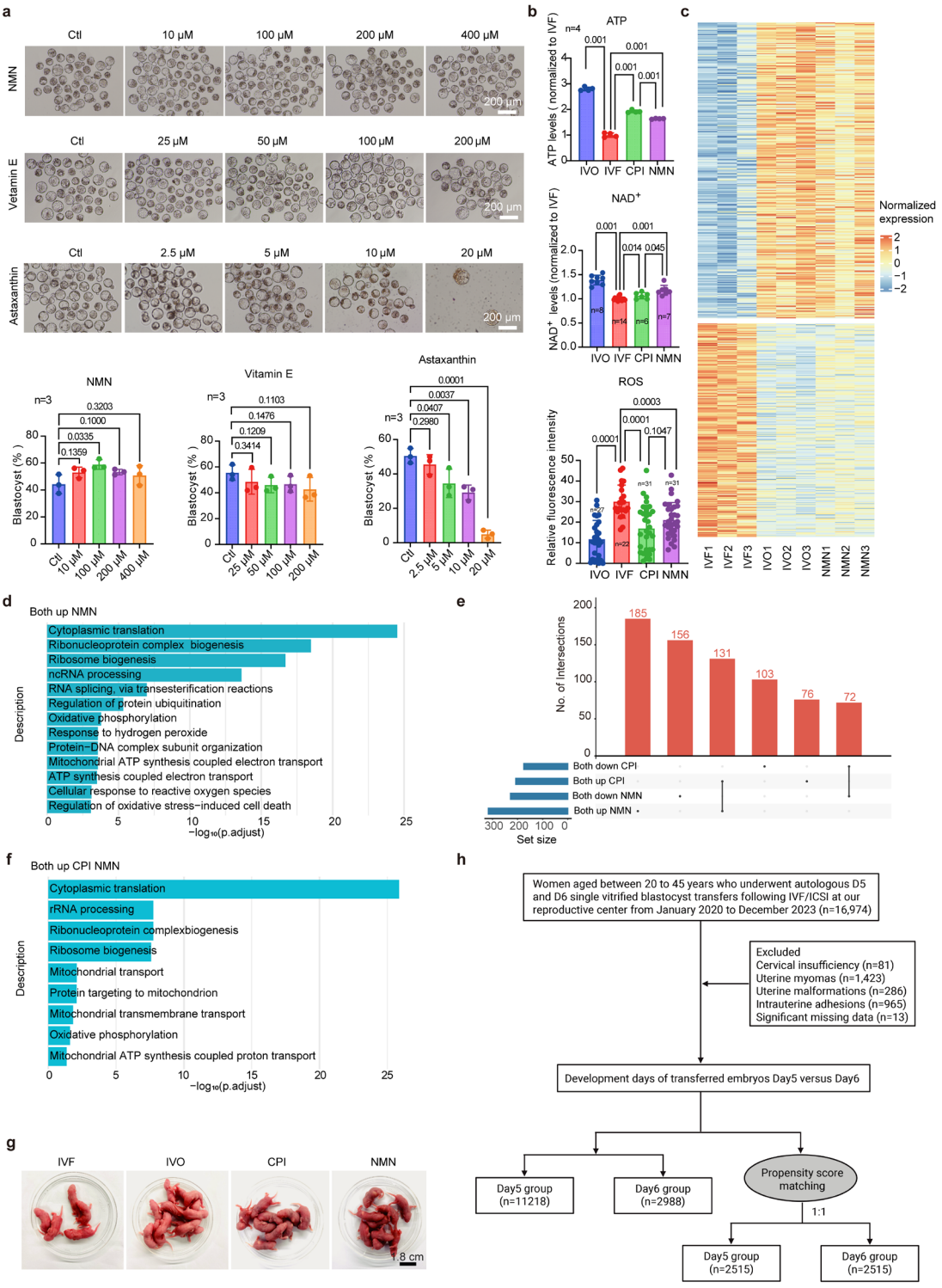

Supplementary Figure 6. The effects of NMN on mouse embryo development. (a) The effects of NMN, vitamin E and astaxanthin on blastocyst formation. Source data are provided as a Source Data file. Error bar: mean± std. Two-tailed unpaired t tests were performed. **(b)** The levels of ATP, NAD+

and ROS in IVO, IVF, CPI-455- and NMN-blastocysts. Source data are provided as a Source Data file. Error bar: mean±std. Two-tailed unpaired t tests were performed. **(c)** Expression heatmap showing the SRGs identified upon NMN treatment. **(d)** Functions of SRGs upon NMN treatment. P-adjust was calculated based on hypergeometric distribution with BH (Benjamini-Hochberg) correction. **(e)** Overlap between SRGs upon CPI-455 and NMN-treatment. **(f)** Functions of SRGs conserved between CPI-455 and NMN-treatment. P-adjust was calculated based on hypergeometric distribution with BH (Benjamini-Hochberg) correction. **(g)** The birth outcome of mice under different conditions including IVF, IVO, CPI-455 and NMN. **(h)** Flow chart for the analysis of clinical outcomes.

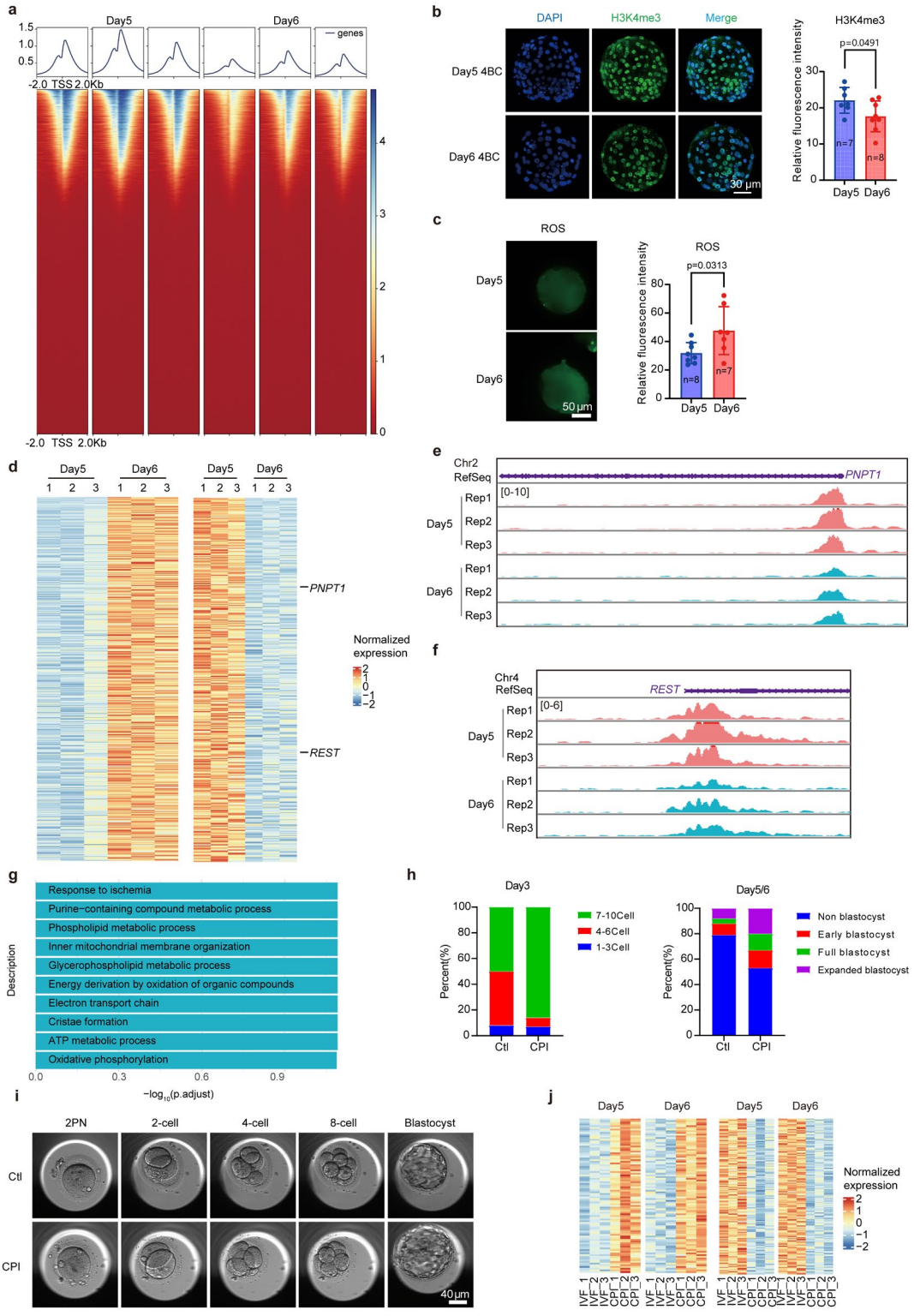

Supplementary Figure 7. The effects of CPI-455 treatment on human embryo development. (a) Heatmaps showing the distribution of H3K4me3 around TSS of human genes in day5- and day6-blastocysts. **(b)-(c)** The staining and quantification of H3K4me3 **(b)** and ROS **(c)** in day5- and day6-

blastocysts. Source data are provided as a Source Data file. Error bar: mean± std. Two-tailed unpaired t tests were performed. **(d)** Heatmaps showing the DEGs identified based on the transcription data of day5- and day6-blastocysts (n = 3 biological replicates for each condition). **(e)-(f)** Two examples showing the down-regulation of *PNPT1* **(e)** and *REST* **(f)** is related to the loss of H3K4me3 at promoter regions. **(g)** Functions of day5-expressed genes. P-adjust was calculated based on hypergeometric distribution with BH (Benjamini-Hochberg) correction. **(h)** Detailed examination of the categories of embryos collected at day3 or day5/6. Source data are provided as a Source Data file. **(i)** Time-lapse images of human embryo *in vitro* cultured with or without CPI-455 treatment. Scale bar, 40 μm. **(j)** Expression heatmaps of CPI-455 sensitive genes (n = 3 biological replicates for each condition).

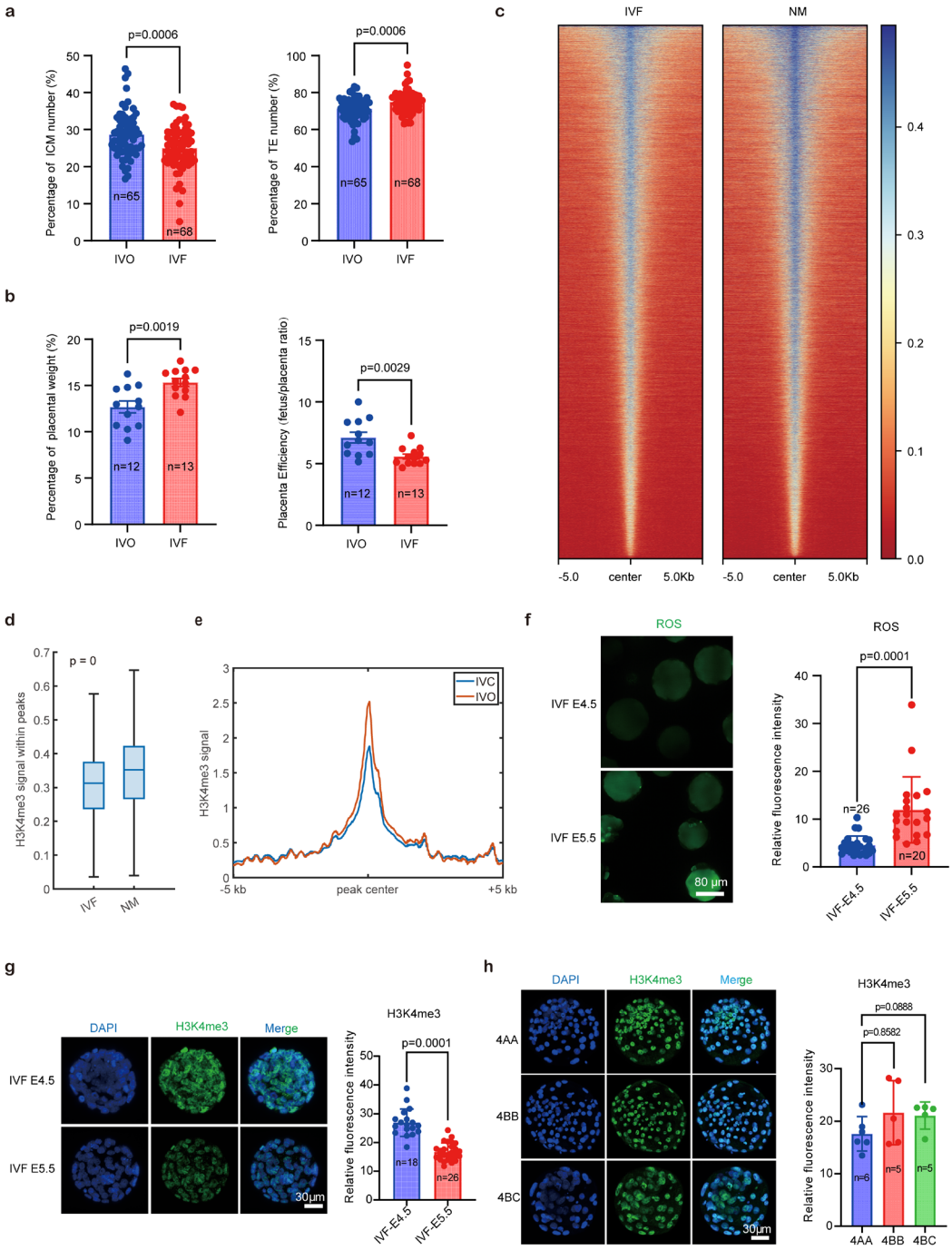

Supplementary Figure 8. The correlation between H3K4me3 and *in vitro* culture time/morphology grade. (a) The proportion of ICM and TE cells in IVF- and IVO-conceived blastocysts. Source data are provided as a Source Data file. Error bar: mean±std. Two-tailed unpaired t tests were performed. **(b)**

The percentage of placental and the efficiency of placenta at E18.5 stage. Source data are provided as a Source Data file. Error bar: mean±std. Two-tailed unpaired t tests were performed. **(c)** Heatmap showing the distribution of H3K4me3 signal around H3K4me3 peaks in IVF and NM. **(d)** Boxplot showing the H3K4me3 signal within H3K4me3 peaks. T-test (both-tail) was performed. The line inside of each box is the sample median and the top and bottom edges of each box are the 0.75 and 0.25 quartiles, respectively. The distance between the top and bottom edges is the interquartile range (IQR). The whiskers are lines that extend above and below each box within 1.5 times the IQR and outliers are values that are more than 1.5 times the IQR away from the top or bottom of the box. **(e)** The distribution of H3K4me3 signal around H3K4me3 peaks in IVC (*in vivo* fertilization and *in vitro* culture) and IVO. **(f)-(g)** The staining and quantification of ROS **(f)** and H3K4me3 **(g)** in E4.5- and E5.5-blastocysts. Source data are provided as a Source Data file. Error bar: mean± std. Two-tailed unpaired t tests were performed. **(h)** The H3K4me3 levels among human day5-blastocysts with different morphological grades. Source data are provided as a Source Data file. Error bar: mean±std. Two-tailed unpaired t tests were performed.

Supplementary table 1. Baseline characteristics and pregnancy outcomes of patients before and after PSM (Propensity Score Matching).

Variables	Before PSM				After PSM			
	Day 5	Day 6	p	t/χ^2	Day 5	Day 6	p	t/χ^2
No. of blastocysts	11218	2988			2515	2515		
Female age (years)	31.16±4.30	32.79±4.62	＜0.001*	-17.362	32.19±4.59	32.44±4.43	0.054	1.925
Body mass index (BMI, kg/m^2)	23.90±3.76	23.97±3.68	0.325	-0.984	23.98±3.67	23.96±3.72	0.858	0.179
Age group , n (%)								
＞35	1662 (14.82)	792 (26.51)	＜0.001*	225.658	640 (25.45)	582 (23.14)	0.057	3.636
≤35	9556 (85.18)	2196 (73.49)			1875 (74.55)	1933 (76.86)		
BMI group, n (%)								
＞24	4970 (44.30)	1359 (45.48)	0.250	1.326	1151 (45.77)	1136 (45.17)	0.671	0.180
⩽24	6248 (55.70)	1629 (54.52)			1364 (54.23)	1379 (54.83)		
Infertility cause, n (%)								
Tubal factor	7844 (69.9)	1839 (61.5)	＜0.001*	90.525	1640 (65.21)	1591 (63.26)	0.146	5.378
Male factor	1877 (16.7)	589 (19.7)			425 (16.90)	484 (19.25)		
Combined	162 (1.4)	41 (1.4)			44 (1.75)	36 (1.43)		
Unexplained	1335 (11.9)	519 (17.4)			406 (16.14)	404 (16.06)		
ART protocol, n (%)								
IVF	8086 (72.08)	1937 (64.83)	＜0.001*	59.774	1704 (67.75)	1679 (66.76)	0.453	0.564
ICSI	3132 (27.92)	1051 (39.17)			811 (32.25)	836 (33.24)		
Full recovered , n (%)	11031 (98.33)	2825 (94.54)	＜0.001*	140.905	2337 (92.92)	2420 (96.22)	＜0.001*	26.683
Hatched , n (%)	9796 (87.32)	2342 (78.38)	＜0.001*	151.743	2042 (80.08)	2031 (80.76)	0.693	0.156

Quality of blastocysts, n (%)								
High (≥4BB)	10573 (94.25)	1979 (66.23)	＜0.001*	1800.595	1898 (75.47)	1890 (75.15)	0.794	0.068
General	645 (5.75)	1009 (33.77)			617 (24.53)	625 (24.85)		
Biochemical pregnancy rate , n (%)	7671 (68.38)	1522 (50.94)	＜0.001*	314.420	1613 (64.14)	1336 (53.12)	＜0.001*	62.890
Clinical pregnancy rate , n (%)	6784 (60.47)	1192 (39.89)	＜0.001*	405.921	1407 (55.94)	1050 (41.75)	＜0.001*	101.405
Ectopic pregnancy , n (%)	52/6784 (0.77)	7/1192 (0.59)	0.505	0.444	6/1407 (0.43)	5/1050 (0.48)	0.855	0.033
Abortion , n (%)	1101/6784 (16.23)	294/1192 (24.66)	＜0.001*	49.987	285/1407 (20.26)	248/1050 (23.62)	0.045*	4.004
Early abortion , n (%)	875/6784 (12.90)	259/1192 (21.73)	＜0.001*	64.817	238/1407 (16.92)	216/1050 (20.57)	0.021*	5.335
Middle and late abortion , n (%)	226/6784 (3.33)	35/1192 (2.94)	0.479	0.500	47/1407 (3.34)	32/1050 (3.05)	0.684	0.166
Live birth rate , n (%)	5631 (50.20)	891 (29.82)	＜0.001*	394.524	1116 (44.37)	797 (31.69)	＜0.001*	85.842
Gestational age (weeks)								
28≤age < 37, n (%)	502/5631 (8.91)	103/891 (11.56)	0.037*	6.263	100/1116 (8.96)	96/797 (12.05)	0.064	5.497
37≤age < 42, n (%)	5126/5631 (91.03)	788/891 (88.44)			1015/1116 (90.95)	701/797 (87.95)		
age≥42, n (%)	3/5631 (0.05)	0/891 (0.00)			1/1116 (0.09)	0/797 (0.00)		

Supplementary table 2. Univariate and multivariate logistic regression analysis on the effect of live birth rate.

	Univariate analysis		Multivariate analysis	
	OR (95% CI)	P Value	OR (95% CI)	P Value
Female age (＞35 VS ≤35)	0.591 (0.514-0.680)	＜0.001*	0.539 (0.458-0.633)	＜0.001*
BMI (＞24 VS ≤24)	0.838 (0.747-0.940)	0.003*	0.863 (0.758-0.984)	0.028*
ART protocol (ICSI VS IVF)	1.167 (1.035-1.317)	0.012*	1.194 (0.950-1.500)	0.129
Blastocyst development day (Day 6 VS Day 5)	0.582 (0.518-0.652)	＜0.001*	0.518 (0.454-0.590)	＜0.001*
Blastocyst quality (General-quality VS High-quality)	0.463 (0.401-0.535)	＜0.001*	0.422 (0.360-0.495)	＜0.001*
Infertility cause (Male factor VS Tubal factor)	1.205 (1.038-1.400)	0.015*	1.010 (0.789-1.292)	0.940
(Combined VS Tubal factor)	1.379 (0.883-2.155)	0.158	-	-
(Unexplained VS Tubal factor)	0.966 (0.823-1.132)	0.668	-	-

Supplementary table 3. The information of human embryos we used in this work.

Type	Stage	Morphological scores	Number	Age and cause of infertility	IVF or ICSI	PGT
ULI-NChIP-seq	Blastocyst	4BB	18	<38，Infertility caused by non-ovarian factors	ICSI	No
WGBS	Blastocyst	4BB	24	<38，Infertility caused by non-ovarian factors	ICSI	No
Smart-seq2 of Day5 and Day6 embryos	Blastocyst	4BB	18	<38，Infertility caused by non-ovarian factors	ICSI	No
CPI-455 Treatment and Smart-seq2	MI	-	256	<38，Infertility caused by non-ovarian factors	ICSI	No
Determination of ROS	Blastocyst	4BB	15	<38，Infertility caused by non-ovarian factors	ICSI	No
Immunofluorescence staining of Day5 and Day6	Blastocyst	4BC	15	<38，Infertility caused by non-ovarian factors	ICSI	No
Immunofluorescence staining in Day5 embryos of different grades	Blastocyst	4AA、4BB、4BC	16	<38，Infertility caused by non-ovarian factors	ICSI	No

Supplementary table 4. The ingredients of IVC1 medium

Reagent name	Vender	Cat No.	Concentration
Advanced DMEM/F-12	Gibco	12634-010	
heat-inactivated FBS	Gibco	16000-044	20%(vol/vol)
200mM L-Glutamine	Thermo Fischer	25030149	2mM
penicillin (25 units/mL)/streptomycin	Gibco	15-140-122	25 μg/mL
100 x ITS-X	Gibco	51500056	1x
β-oestradiol	sigma	E2758	8 nM
progesterone	sigma	P0130	200 ng/ml
N-acetyl-l-cysteine	sigma	A7250	25 μM
RGF BME, Type 2	R&D Systems	3533-005-02	0-20%(vol/vol)

Supplementary table 5. The ingredients of IVC2 medium

Reagent name	Vender	Cat No.	Concentration
Advanced DMEM/F-12	Gibco	12634-010	
KOSR	Thermo Fischer	A3181501	30%(vol/vol)
200mM L-Glutamine	Thermo Fischer	25030149	2mM
penicillin (25 units/mL)/streptomycin	Gibco	15-140-122	25 μg/mL
100 x ITS-X	Gibco	51500056	1x
β-oestradiol	sigma	E2758	8 nM
progesterone	sigma	P0130	200 ng/ml
N-acetyl-l-cysteine	sigma	A7250	25 μM
RGF BME, Type 2	R&D Systems	3533-005-02	0-20%(vol/vol)

Supplementary table 6. The information of antibodies used in immunofluorescence

Reagent name	Vender	Cat No.
anti-CARM1	Cell Signaling Technology	12495S
anti-OCT4	Santa Cruz Biotechnology	sc5729
anti-CDX2	Abcam	ab76541
anti-EOMES	Abcam	ab23345
anti-GATA4	Abcam	ab84593
anti-TET3	Proteintech	22612-1-AP
anti-H3K4me3	Cell Signaling Technology	9751T
anti-H3K27me3	Active motif	39155
Mounting Medium with DAPI	Abcam	ab104139
Goat Anti-Mouse IgG H&L (Alexa Fluor 488) preadsorbed	Abcam	ab150117
Goat Anti-Mouse IgG H&L (Alexa Fluor 594) preadsorbed	Abcam	ab150120
Goat Anti-Rabbit IgG H&L (Alexa Fluor 488) preadsorbed	Abcam	ab150081
Goat Anti-Rabbit IgG H&L (Alexa Fluor 647) preadsorbed	Abcam	ab150083
Donkey Anti-Goat IgG H&L (Alexa Fluor 594) preadsorbed	Abcam	ab150136

Supplementary table 7. The primer sequences of RT-qPCR

Primer	Sequence (5'- 3')
Carm1-F	CCTATCCCAGCAGCAGAAC
Carm1-R	GAGCCACAGCCCACATC
Atp5h-F	GCTGGGCGTAAACTTGCTCTA
Atp5h-R	CAGACAGACTAGCCAACCTGG
Tomm5-F	ATGAAGCGGAAGATGCGTGAG
Tomm5-R	AGGGCCACGTAGATGAGGAA
Atp5j2-F	TGCCGAGCTGGATAATGATGC
Atp5j2-R	ACCATGCTAATCCCCGAGATG
Mgarp-F	GAAGGACGCATCTCTTCGCC
Mgarp-R	GCAACTCCGCCTTTGTTTGTT
Hspd1-F	CACAGTCCTTCGCCAGATGAG
Hspd1-R	CTACACCTTGAAGCATTAAGGCT
Tomm7-F	ATCCGCTGGGGCTTTATTCC
Tomm7-R	CGACGGTTCAGGCATTCCA
Txn1-F	CATGCCGACCTTCCAGTTTTA
Txn1-R	TTTCCTTGTTAGCACCGGAGA
Rnf146-F	GTTATCTGTGTGTAAAGGGTGCT
Rnf146-R	CTGGTGACAACAAGGTTGGCT
Commd1-F	CTGCACAGCCAACTCTATCCG
Commd1-R	GCCTCTAACTGGTTGAAATCCA
Rps7-F	AGCGCCAAGATCGTGAAGC
Rps7-R	CACCACCAACTTCGATTTCCTT
Rpl11-F	ATGGCGCAAGATCAAGGGG
Rpl11-R	GACTGTGCAGTGAACAGCAAT
Rpl23-F	TTCCGGTCGGAGCTGTGAT
Rpl23-R	CTGCTGGATGTACCTTTTTCCTT
Rpl37-F	CATCCTTTGGTAAGCGTCGCA
Rpl37-R	TGGCACTCCAGTTATACTTCCT
Gapdh-F	CCTTCCGTGTTCCTACCC
Gapdh-R	CAACCTGGTCCTCAGTGTAG

Supplementary table 8. The sequencing depth after down-sampling

Groups	Sequencing depth (M: million)
D5 vs D6 (H3K4me3)	19.5 M
IVF vs IVO (H3K4me3)	33 M
IVF vs IVO (H3K27me3)	32 M
IVF vs IVO vs CPI-455 (H3K4me3)	24 M